EXPERIMENTAL STUDY ON CYCLIC BOND BEHAVIOR BETWEEN CFRP AND STEEL

Qian-Qian Yu, Tongji University, China, qianqian.yu@tongji.edu.cn
Hai-Bin Xu, Tongji University, China, 1932535@tongji.edu.cn

ABSTRACT
Bond behaivor between carbon fiber-reinforced polymer (CFRP) and steel is recognized important to ensure load transfer and consequently retrofitting efficiency in external bonding repair schemes. This study presents an experimental study on CFRP-to-steel single-lap shear joints subjected to cyclic loading. Various fatigue loading amplitudes were considered. All the specimens fractured by cohesive failure. Fatigue life of the samples gradually reduced with the increased loading levels. With the fatigue cycles elapsed, the bond stiffness declined whereas the residual slip increased. Development of the damage index versus the normalized fatigue cycle number was derived, which was approximately the same among the scenarios with various loadings.

KEYWORDS
CFRP; steel interface; bond; cyclic

INTRODUCTION
Fatigue damage is a major concern of steel structures, which leads to 50−90% mechanical failure (Stephens et al., 2000). Subjected to service loads and environmental agents, cracks may initiate and develop in zones of stress concentration, even leading to catastrophic accidents. In comparison with demolition and reconstruction, retrofitting and rehabilitation of aged structures are recognized as a more economic and environmentally friendly way. Carbon fiber-reinforced polymer (CFRP) materials with excellent mechanical properties, i.e., high strength-to-weight ratio, good resistance to fatigue and corrosion, and ease of installation, nowadays is attracting much attention and has been extensively applied in concrete and masonry structures. In terms of steel structures, it has been demonstrated that CFRP materials could be employed to effectively improve performance of damaged steel structures as well as to retard crack propagation and consequently to extend fatigue life (Zhao and Zhang, 2007; Yu et al., 2013&2017).

A good bond performance between CFRP and substrate plays an important role in external bonding repair scheme, which determines utilization rate of CFRP materials. Generally, CFRP externally bonded to steel substrate may fail in six patterns (Zhao and Zhang, 2007). Although extensive studies have been carried out to evaluate the interfacial behavior between CFRP and steel (Hart-Smith, 1973; Xia and Teng, 2005; Fernando et al., 2014; He and Xian, 2016; Wang and Wu, 2018; Yu et al., 2012), to the best of the authors' knowledge, scenarios of the bond behavior subjected to fatigue loading has not been fully understood and examination of fatigue retrofitting of steel structures by using CFRP materials is more frequently relied on the monotonic behavior between CFRP and steel (Liu et al., 2010; Yang et al., 2018; Yu et al., 2018; Wang et al., 2019; Pang et al., 2019).

In Zhang et al. (2019), a series tests on CFRP-to-steel double-shear specimens were conducted. The interfacial crack propagation rate increased with the increment of the stress ratio or stress level. Eventually, an empirical formula of *S*-*N* curve of the joints was proposed. More recently, Doroudi et al. (2020) performed fatigue test on CFRP-to-steel single-lap shear joints. A damaged-plasticity-type bond-slip relation was developed to model the constitutive behavior of the bonded interface under quasi-static cyclic loading.

This study investigates the bond behavior between CFRP and steel subjected to fatigue loading. Single lap-shear specimens were tested, and different stress ratios of the fatigue spectrum were considered. The fatigue life, load-displacement and damage in the bond stiffness was carefully recorded and discussed.

EXPERIMENTAL PROGRAM

The test program was conducted in Key Laboratory of Performance Evolution and Control for Engineering Structures (Tongji University). A total of 14 specimens were prepared, of which two were tested under monotonic loading and 12 were intended to investigate the bond behavior loaded under fatigue.

Specimen configuration and geometry

A single-lap shear test setup was adopted in the experimental program. Figure 1 illustrates the configuration and geometry of the specimens. The steel substrate was 400 mm long, 140 mm wide and 10 mm thick. A CFRP strip with a width of 50 mm and a length of 630 mm was attached on it.

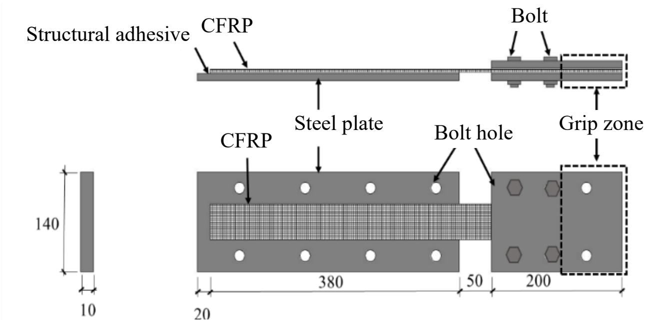

Figure 1: Configuration and dimensions of the test specimen (unit in mm, not to scale)

A sufficient effective bond length, i.e., 380 mm was selected here to ensure bond performance (Xia and Teng 2005). The bond thickness was controlled around 0.5 mm. Eight bolt holes were set on the steel substrate which was designed to be mounted to the test frame. The load end of the CFRP was bonded to two steel plates connected by four bolts. The bond areas of the steel substrate were first sandblasted to roughen the surfaces and to remove the weak surface layer, thus providing a chemically-active rough surface for adhesive bonding. All the specimens were cured for 14 days in room condition before testing.

Material properties

The steel plates used in the tests were Q355B (GB 50017-2003, 2003). Tensile coupon tests were conducted to determine the mechanical properties (AS1391, 1991). The average yield strength, ultimate tensile strength, and Young's modulus were 367 MPa, 493.0 MPa, and 207 GPa, respectively. CFRP laminates were provided in rolls with a width of 50 mm and its nominal thickness was 1.4 mm. The mechanical properties were also obtained from flat coupon tests (ASTM D3039-08, 2008). The CFRP strip, with fibers unidirectional, exhibited a Young's modulus of 164 GPa, an ultimate tensile strength of 2598 MPa, and an ultimate strain of 17200 με. Structural adhesive Araldite 2015 was adopted to bond the CFRP to the steel substrate. The measured Young's modulus and ultimate strength according to ASTM D638-10 (2010) were 1.42 GPa and 18.47 MPa, respectively.

Test set-up

The specimen was attached to a loading frame which was used to fix the steel substrate and tensile load was applied to grip zone. In this way, the samples were loaded in mode II shear. An MTS 322 servo-hydraulic testing machine was adopted to apply fatigue loading. In the monotonic test, the displacement control with a loading rate of 0.003 mm/s was selected whereas in the cyclic test, the load control with a frequency of 10 Hz and a stress ratio *R* (minimum load to maximum load) of 0.1 was used. Strain gauges with an interval of 25 mm were attached on the surface of CFRP to characterize the strain variation during loading (Figure 2).

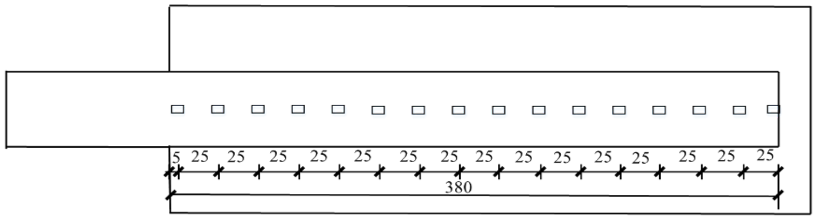

Figure 2: Layout of strain gauges on the CFRP (unit in mm, not to scale)

TEST AND DISCUSSIONS

The test program and results are summarized in Table 1. The specimen nomenclature is as follows: M = monotonic loading; C = cyclic loading. The number after the hyphen represents the stress ratio, which was defined as the ratio of the maximum load in fatigue to the average static bond strength. The final number indicates the two identical specimens tested for one scenario.

Table 1: Experimental program and results

Specimen	Load	Bond thickness (mm)	Load ratio	Ultimate load or fatigue life
M-1	Monotonic	0.53	/	98.85 kN
M-2	Monotonic	0.55	/	93.66 kN
C-0.3-1	Cyclic	0.52	0.3	455598
C-0.3-2	Cyclic	0.53	0.3	319946
C-0.4-1	Cyclic	0.51	0.4	73792
C-0.4-2	Cyclic	0.54	0.4	49194
C-0.5-1	Cyclic	0.54	0.5	7303
C-0.5-2	Cyclic	0.52	0.5	14846
C-0.6-1	Cyclic	0.55	0.6	2403
C-0.6-2	Cyclic	0.53	0.6	3376
C-0.7-1	Cyclic	0.55	0.7	1147
C-0.7-2	Cyclic	0.53	0.7	1339
C-0.8-1	Cyclic	0.51	0.8	468
C-0.8-2	Cyclic	0.54	0.8	660

Failure mode

Cohesive failure was observed for all the specimens regardless of the loading type (Figure 3). Debonding gradually propagated from the loading end to the free end, till final fracture for both cased under static and fatigue loading. In comparison with specimens subjected to monotonic load, the fracture surface exhibited smoother in the samples loaded by fatigue. It was mainly because friction between the CFRP patch and the steel substrate during fatigue. In addition, it was expected that the samples with lower fatigue loading and consequently longer fatigue life led to a smoother facture surface.

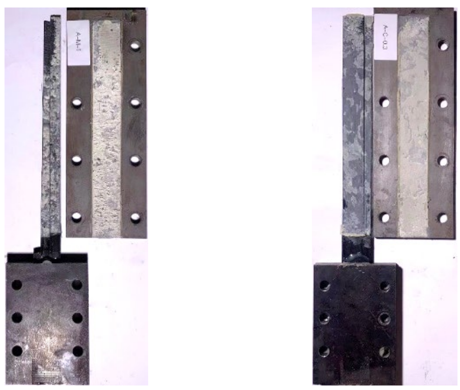

(a) A-M-1 (b) C-0.3-1

Figure 3: Failure mode of the specimens

Fatigue life

The fatigue life of the specimens was counted in the test when the CFRP strip was pull off from the steel substrate, and is listed in Table 1. As the load ratio was increased from 0.3 to 0.8, the average fatigue life of the specimens were significantly decreased from 387772 to 564. The logarithm of the fatigue life generally displayed a linear relationship with the load ratio (Figure 4), which was in conformance with experimental finding reported in Wang et al., (2019). The regressed equation is given as follows.

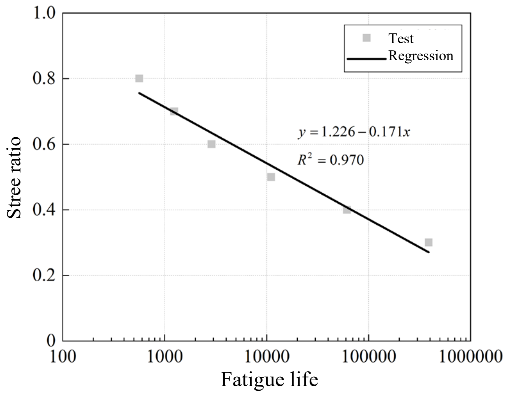

Figure 4: Stress ratio versus fatigue life of the specimens

$$m = -0.171 \times \log_{10} N + 1.226 \qquad \text{Eq. 1}$$

$$N = 10^{\frac{m-1.226}{-0.171}} \qquad \text{Eq. 2}$$

where N is the fatigue life and m is the stress ratio.

Load-displacement curves

Figure 5 plots typical load-displacement curves of the specimen C-0.4-2. As the number of fatigue cycles elapsed, the displacement at the loading end of the specimen increased, and the stiffness gradually decreased, indicating the accumulative damage to the bond interface. The area enveloped by the loading and unloading curves indicated the energy dissipation.

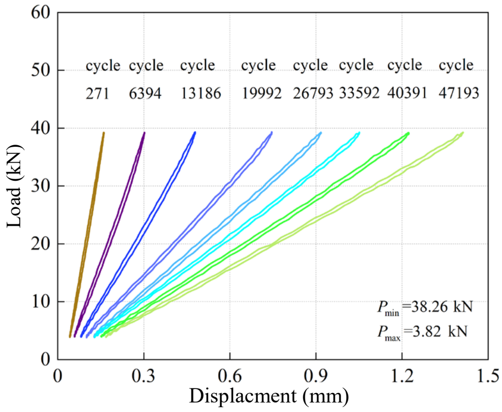

Figure 5: Load-displacement curves of the specimen C-0.4-2

The stiffness of the bond interface was then obtained

$$K(n) = \frac{P_{max} - P_{min}}{s_{max} - s_{min}} \qquad \text{Eq. 3}$$

where P_{max} and P_{min} are the maximum and minimum load in the fatigue spectrum, respectively. s_{max} and s_{min} denote the displacement at the loading end at P_{max} and P_{min}, respectively. $K(n)$ is the stiffness at the fatigue cycle number of n.

A parameter D was introduced to describe the reduction of the bond stiffness, as shown in Eq. (4)

$$D(n) = \frac{K(1) - K(n)}{K(1)} \quad \text{Eq. 4}$$

where $K(1)$ is the initial bond stiffness, $K(n)$ is the n^{th} bond stiffness, and $D(n)$ represents the bond damage in the n^{th} fatigue cycle.

Figure 6 illustrates the damage index D versus the normalized fatigue life. It should be pointed out that, five specimens were missed from the figure due to the damaged strain gauges and consequently lost slip values. Variation of the damage index D of different specimens generally followed the same path. It first quickly increased with the normalized fatigue life and then gradually slowed down. When approaching failure, D values of all the samples approximately reached 0.9.

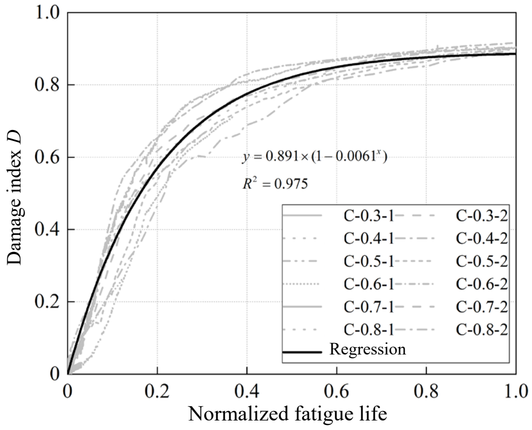

Figure 6: Damage index D versus normalized fatigue life

A regressed equation represents the relationship between the damage index and the normalized fatigue life of all the specimens is give as follows

$$D(n/N_f) = 0.891 \times \left(1 - 0.0061^{(n/N_f)}\right) \quad \text{Eq. 5}$$

where N_f is the fatigue life of the specimen.

CONCLUSIONS

In this study, an experimental study was conducted to investigate the bond behavior between CFRP and steel subjected to cyclic loading. Stress ratios ranging from 0.3 to 0.8 was selected. All the specimens fractured by cohesive failure regardless of the loading specturem. Fatigue life of the samples gradually reduced with the increased loads, and the logarithm of the fatigue life generally displayed a linear relationship with the stress ratio. With the fatigue cycles elapsed, the bond stiffness declined whereas the displacement at the loading end increased. Evolution of the damage index versus the normalized fatigue cycle number was derived, which firstly quickly increased with the cyclic loadings and then gradually slowed down. Damage in the bond stiffness of specimens with different loading histories exhibited an approximately variation trend.

REFERENCES

AS 1391-1991 (1991). Methods of Tensile Testing of Metals, Standards Australia.

ASTM D3039-08 (2008). Standard Test Method for Tensile Properties of Polymer Matrix Composite Materials. ASTM International.

ASTM D638-10 (2010). Standard Test Method for Tensile Properties of Plastics. ASTM International.

Doroudi, Y., Fernando, D., Zhou, H., Nguyen, V. T. & Ghafoori, E. (2020). Fatigue behavior of FRP-to-steel bonded interface: An experimental study with a damage plasticity model. *International Journal of Fatigue*, 139: 105785.

Fernando, D., Yu, T., Teng, J.G. (2014). Behavior of CFRP laminates bonded to a steel substrate using a ductile adhesive. *Journal of Composite for Construction*, 18(2): 04013040.

GB 50017-2003 (2003). Code for Design of Steel Structures, Standards China.

Hart-Smith, L. (1973). Adhesive-bonded double-lap joints. NASA contract report.

He, J., & Xian, G. J. (2016). Debonding of CFRP-to-steel joints with CFRP delamination. *Composite Structures*, 153: 12-20.

Liu, H. B., Zhao, X. L., & Al-Mahaidi, R. (2010). Effect of fatigue loading on bond strength between CFRP sheets and steel plates. *International Journal of Structural Stability and Dynamics*, 10(1): 1-20.

Pang, Y. Y., Wu, G., Wang, H. T., Su, Z. L., & He, X. Y. (2019). Experimental study on the bond behavior of CFRP-steel interfaces under quasi-static cyclic loading. *Thin-Walled Structures*, 140: 426-437.

Stephens, R. I., Fatemi, A., Stephens, R. R., & Fuchs, H. O. (2000). Metal Fatigue in Engineering, Second Edition John Wiley & Sons Inc.

Wang, H. T., & Wu, G. (2018). Bond-slip models for CFRP plates externally bonded to steel substrates. *Composite Structures*, 184: 1204-1214.

Wang, H. T., Wu, G., Pang, Y. Y., Shi, J.W., & Zakari, H.M. (2019). Experimental study on the bond behavior between CFRP plates and steel substrates under fatigue loading. *Composites Part B*, 176: 107266.

Xia, S. H., & Teng, J. G. (2005). Behaviour of FRP-to-steel bonded joints. *Proceedings of the international symposium on bond behaviour of FRP in structures (BBFS 2005)*, Hong Kong, China.

Yang, Y. M., Silva, M. A. G., Biscaia, H., & Chastre, C. (2018). CFRP-to-steel bonded joints subjected to cyclic loading: An experimental study. *Composites Part B*, 146: 28-41.

Yu, T., Fernando, D., Teng, J. G., & Zhao, X. L. (2012). Experimental study on CFRP-to-steel bonded interfaces. *Composites Part B*, 43(5): 2279-2289.

Yu, Q. Q., Chen, T., Gu, X. L., Zhao, X. L., & Xiao, Z.G. (2013). Fatigue behaviour of CFRP strengthened steel plates with different degrees of damage. *Thin-Walled Structures*, 69: 10-17.

Yu, Q. Q., & Wu, Y. F. (2017). Fatigue strengthening of cracked steel beams with different configurations and materials. *Journal of Composites for Construction*, 21(2): 04016093.

Yu, Q. Q., Gu, X. L., Zhao, X. L., Zhang, D. M., Huang, H. W., &Jiang, C. (2019). Characterization of model uncertainty of adhesively bonded CFRP-to-steel joints. *Composite Structures*, 215: 150-165.

Yu, Q. Q., Gao, R. X., Gu, X. L., Zhao, X. L., & Chen T. (2018). Bond behavior of CFRP-steel double-lap joints exposed to marine atmosphere and fatigue loading. *Engineering Structures*, 175: 76-85.

Zhang, L., Cao, S. Y., & Tao, X. (2019). Experimental study on interfacial bond behavior between CFRP sheets and steel plates under fatigue loading. *Materials*, 12(3): 377.

Zhao, X. L., & Zhang, L. (2007). State-of-the-art review on FRP strengthened steel structures. *Engineering Structures*, 29(8): 1808-1823.

ACKNOWLEDGEMENT

This study was supported by the National Natural Science Foundation of China (Project Nos. 52222803 and 51878485).

CONFLICT OF INTEREST

The authors declare that they have no conflicts of interest associated with the work presented in this paper.

DATA AVAILABILITY

Data on which this paper is based is available from the authors upon reasonable request.